DOI: 10.1002/anie.201209929

Molecular Imaging of Paintings

Noninvasive Analysis of Paintings by Mid-infrared Hyperspectral Imaging**

Francesca Rosi, Costanza Miliani, René Braun, Roland Harig, Diego Sali, Brunetto G. Brunetti, and Antonio Sgamellotti*

In recent years, in situ noninvasive spectroscopy has played an increasingly important role in art conservation. Spectroscopic methods can be used to gain a deep understanding of the material composition of art objects while fully respecting their integrity and value. Considerable improvements in detector technology, instrument–computer interfacing, focusing optics, and the performance of radiation sources have been made in the spectroscopic field and have led to the development and successful application of a series of noninvasive and portable analytical tools for point examination.[1–6]

In this context, current scientific interest is focused on the development of mapping/imaging multi-/hyperspectral methods, since area examination naturally meets the demands of a holistic art-historical approach by revealing not only the chemical composition of painting materials but also their semiquantitative spatial distribution with respect to what is visible to the naked eye.[7] Recently, the possibility of mapping elemental distribution on paintings by means of a portable scanning macro X-ray fluorescence device was demonstrated to be useful for the investigation of the materials used by artists.[8] The molecular identification and spatial distribution of a number of pigments can be inferred from reflection imaging in the visible (Vis: 400–750 nm) and near-infrared regions (NIR: 750–2500 nm) by combining information on electronic transitions in the visible range with overtone and combination vibrational bands in the near-infrared range which are associated with inorganic pigments containing hydroxy groups, such as lead white, azurite, and gypsum.[9]

[*] Dr. F. Rosi, Dr. C. Miliani
Istituto di Scienze e Tecnologie Molecolari CNR-ISTM, SMAArt
Via Elce di sotto, 9 Perugia 06123 (Italy)
E-mail: costanza.miliani@cnr.it
D. Sali
Bruker Italia Srl Unipersonale
Viale Vincenzo Lancetti 43, 20158 Milan (Italy)
R. Braun, Dr. R. Harig
Bruker Optics
Rudolf-Plank-Strasse 27, 76275 Ettlingen (Germany)
Prof. B. G. Brunetti, Prof. A. Sgamellotti
SMAArt, Dipartimento di Chimica, Università di Perugia
Via Elce di sotto, 9 Perugia 06123 (Italy)

[**] We thank the Fondazione Albizzini for allowing access to the Burri Collection and A. Daveri for help in data collection. We acknowledge financial support from the European Commission (FP7 Research Infrastructures, CHARISMA GA no. 228330), MIUR (PRIN08, Materiali e sistemi innovativi per la conservazione dell'arte contemporanea, 2008 FFXXN9), and the Associazione Laboratorio di Diagnostica di Spoleto.

The identification and mapping of organic compounds is a challenge for the noninvasive analysis of artworks. In comparison with inorganic pigments and fillers, there is a larger variety of organic compounds, and they are present in smaller amounts and more subject to chemical alteration. If both traditional and modern art are taken into consideration, just some of the organic compounds to be identified and localized may include: drying oils, proteins, acrylics, alkyds, polyvinyl acetates, natural and synthetic waxes, terpene resins, and natural and synthetic dyes. Recently, Ricciardi et al. demonstrated the potential of hyperspectral imaging in the NIR region (10000–4000 cm^{-1}) to discriminate between lipid and proteinaceous binders on illuminated manuscripts[10] on the basis of the vibrational combination/overtone bands of methylene groups and amides.[11] In contrast, the mid-infrared (MIR) range has not yet been exploited for the spatially resolved remote study of artworks, although the MIR range (4000–600 cm^{-1}) has proved to be very informative for the identification of artists' materials by noninvasive point analysis[5,6,12] or microinvasively by cross-section imaging.[13]

Herein, we describe the potential of imaging MIR spectroscopy for painting analysis through the application of a novel hyperspectral imaging system (HI90, Bruker Optics). The system developed for the remote identification and mapping of hazardous compounds[14–16] was adapted in this study for reflection measurements of paintings by the use of an external infrared radiation source. The subject of our study was a painting by Alberto Burri, *Sestante 10* (1982), which is currently exhibited at the Ex-Seccatoi del Tabacco (Perugia, Italy).

Three areas (ca. $9 \times 9\ cm^2$) of the large painting ($250 \times 360\ cm^2$) were analyzed on site with the HI90 system. We also investigated several points within the same areas noninvasively with a portable FTIR spectrometer (Alpha-R, Bruker Optics) to validate the assignment made on the basis of the HI90 spectral data.

In Figure 1 a, the visible image of the investigated area I of *Sestante 10* is shown. The resulting brightness temperature difference images in Figure 1 b,c clearly highlight the use of a different binder for the orange sector to that used for the other sectors. More precisely, the image depicted in Figure 1 b shows the false-color representation of the difference in the mean brightness temperature for a peak in the signature of the orange area (1154–1167 cm^{-1}) and the mean brightness temperature for a frequency range in which the reflectance is lower (1197–1209 cm^{-1}; see range (b) in Figure 1 d). The area in the brightness temperature image in Figure 1 b indicates the presence of an acrylic binder, as suggested by a comparison with the spectrum recorded with the HI90 instrument

© 2013 Wiley-VCH Verlag GmbH & Co. KGaA, Weinheim

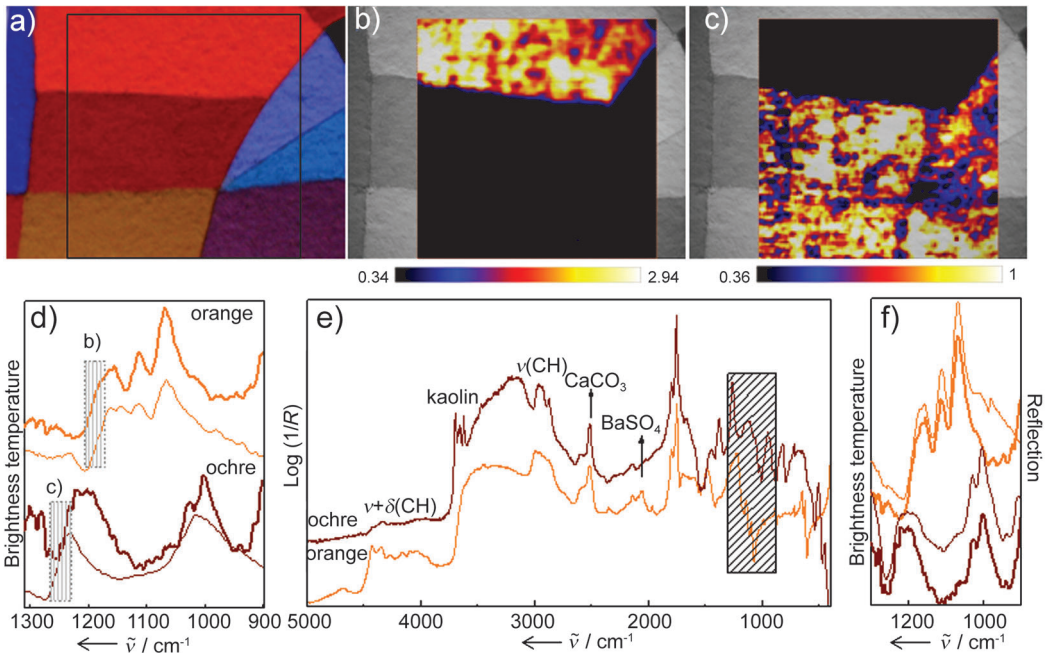

Figure 1. a) Color image of a portion of the painting *Sestante 10* by Burri. The black rectangle highlights the area investigated with the HI90 system (area I, ca. 9×9 cm^2). b) False-color representation of the difference in the mean brightness temperature (measured in Kelvin) between 1154 and 1167 cm^{-1} and the mean brightness temperature between 1197 and 1209 cm^{-1}. c) False-color representation of the difference in the mean brightness temperature (measured in Kelvin) between 1250 and 1255 cm^{-1} and the mean brightness temperature between 1220 and 1230 cm^{-1}. d) Comparison of the spectral profiles representative of the two areas highlighted in (b) and (c) with reference spectra collected with the HI90 imager from laboratory paint models composed of lithopone white and acrylic resin (thin orange line) and a silica-based pigment with a vinyl binder (thin wine-colored line). e) Infrared reflection spectra acquired with the Alpha-R spectrometer for the orange and ochre sectors over the whole accessible spectral range (the rectangle highlights the range investigated with the HI90 imager). f) Comparison of the spectral profiles obtained with the HI90 instrument (thick lines) and the Alpha-R spectrometer (thin lines) in the orange and ochre sectors.

from a laboratory sample of lithopone white and acrylic resin (Figure 1 d). The presence of an acrylic medium is clearly confirmed by the point-analysis spectrum (Figure 1 e), which shows the combined presence of signals at about 1170 cm^{-1} (derivative shape), the characteristic shape of CH stretching bands at 2900 cm^{-1},[16] and the combination ν + δ(CH) in the NIR region. The distribution shown in Figure 1 c was obtained by considering the brightness temperature change in the range 1200–1250 cm^{-1} (see range (c) in Figure 1 d) and indicates the use of a vinyl binder common to the red, ochre, blue, cyan, and purple sectors. Again, the results were validated by point analysis (Figure 1 e), which showed the presence of a band at 1260 cm^{-1} and CH stretching bands around 2900 cm^{-1} and thus confirmed the presence of a vinyl medium.[6] The excellent quality of the spectra collected by the hyperspectral imaging system is evident in Figure 1 f, in which the HI90 brightness temperature profiles are compared with the corresponding Alpha-R reflection spectra.

We used the same approach to investigate area II of *Sestante 10* (Figure 2 a). Similar spectral ranges were considered for imaging the binder distribution in the two brightness temperature difference images in Figure 2 b,c. Brightness temperature changes observed for the light-green sector in the 1100–1200 cm^{-1} range suggest the use of an acrylic binder (Figure 2 d). In contrast, the blue, dark-green, and purple sectors were probably painted with a vinyl binder characterized by bands in the 1200–1250 cm^{-1}range. These considerations were more properly confirmed by comparing the brightness temperature profiles of the two sectors with those acquired with the HI90 instrument on laboratory paint models (Figure 2 d). The overall imaging results are validated by the corresponding point analysis, which, on the basis of the previously discussed bands observed for area I, highlights the certain presence of an acrylic binder for the light-green sectors and a vinyl resin for the dark-green area (Figure 2 e).

These findings validate the chemical images obtained on the basis of the bands observed for the two binders in the spectral range of the HI90 instrument in the configuration used for this study. The strength of the imaging approach used for the localization of the two organic binders certainly arises from the remarkable spectral quality of the hyperspectral images, as shown in Figure 2 f, in which the spectra from the imaging system are compared with those collected by the point spectrometer. Point analysis in the extended spectral range revealed the presence of further signals related to some inorganic components, namely, pigments and fillers whose distribution in the painting is also important. With the aim of visualizing the distribution of these inorganic components, a third area was studied with the HI90 instrument. The investigated area III (ca. 9×9 cm^2) is shown in Figure 3 a and mainly corresponds to area II discussed above. Reflection spectra acquired with the FTIR spectrometer were used as reference data to calculate the correlation coefficient of the HI90 data, pixel by pixel. Figure 3 b–e depicts graphically the correlation coefficient between the measured and reference spectra. The resulting correlation images display the distribution of four different spectral profiles in the investigated area. As indicated by the brightness temperature spectra (Figure 3 f), the purple area is characterized by the combined presence of a silicate pigment (Si–O antisymmetric band at ca. 1000 cm^{-1} [12]) and calcium sulfate (SO_4^{2-} antisymmetric band at ca. 1150 cm^{-1} [12]). The dark-green sector differs from the

© 2013 Wiley-VCH Verlag GmbH & Co. KGaA, Weinheim

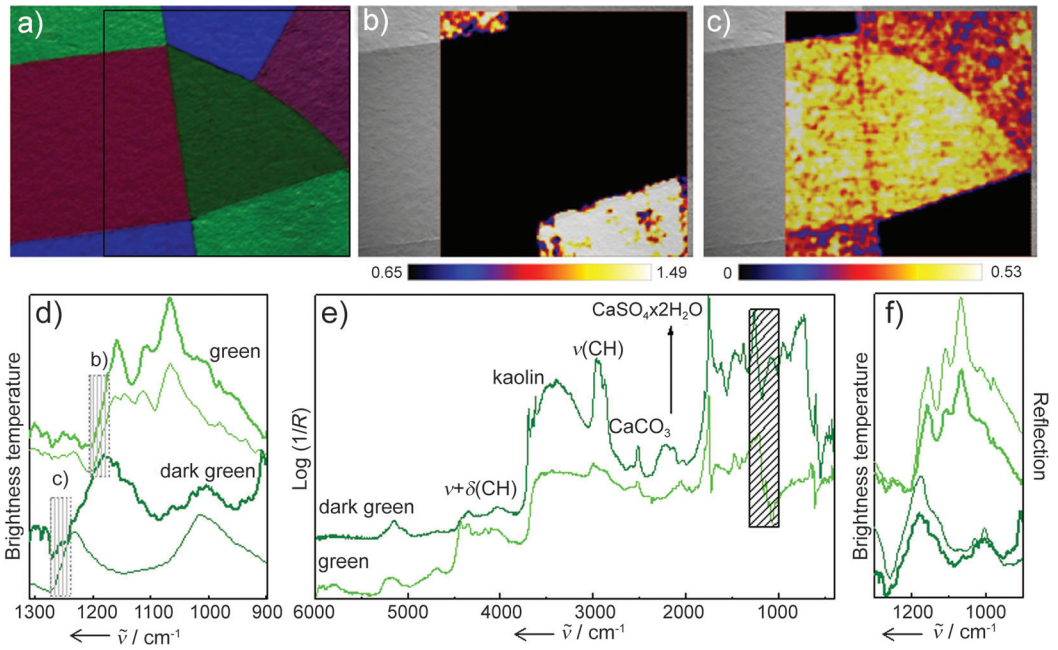

Figure 2. a) Color image of a portion of the painting *Sestante 10* by Burri. The black rectangle highlights the area investigated with the HI90 system (area II, 9×9 cm^2). b,c) Brightness temperature difference images (measured in Kelvin) in the range 1155–1159 to 1200–1203 cm^{-1} (b) and 1209–1215 to 1243–1249 cm^{-1} (c). d) Comparison of the spectral profiles representative of the two areas highlighted in (b) and (c) with reference spectra collected with the HI90 imager from laboratory paint models composed of lithopone white and acrylic resin (thin green line) and a silica-based pigment with a vinyl binder (thin dark-green line). e) Infrared reflection spectra acquired with the Alpha-R system with spectral assignment in the whole spectral range accessible with the portable spectrometer for the green and dark-green sectors (the rectangle highlights the portion of the range accessible with the HI90 instrument). f) Comparison of the spectral profiles obtained with the HI90 instrument (thick lines) and the Alpha-R system (thin lines) in the green and dark-green sectors.

light-green sector not only in the binder but also in the inorganic component (Figure 3c,d). In fact, the typical three-band profile in the range 1040–1180 cm^{-1} of the brightness temperature profiles (Figure 3f) clearly indicates the presence of barium sulfate,[12] which was probably used to lighten the green hue and is not present in the dark-green area, in which only a silicate component was identified.

Finally, the blue sector is characterized by a band at about 1000 cm^{-1}, which in combination with the shoulder visible at 1030 cm^{-1} indicates the presence of a silicate pigment. These results were confirmed by point-analysis measurements, which clearly showed the presence of kaolin, not only in the blue but also in the purple and dark-green sectors, as indicated by the band at 1000 cm^{-1} (Figure 2e). Furthermore, point investigation indicated the presence of gypsum, not only in the purple area as also suggested by the results obtained with the HI90 instrument, but also in the dark-green area.

In conclusion, the present study clearly provides evidence for the high potential of mid-IR imaging for the study of painting materials with a novel hyperspectral imaging system. The stand-off hyperspectral imaging of a surface on the basis of the highly informative range of the IR fingerprint region opens up new broad perspectives for the noninvasive analysis of artworks.

Experimental Section

The hyperspectral imager HI90 is based on the combination of a Michelson interferometer with a focal-plane-array (FPA) mercury cadmium telluride (MCT) detector. The plane-mirror interferometer was actively aligned. The maximum lateral resolution was 256×256 pixels, and cooling was performed by a Stirling cooler. The configuration applied in this study operates in the spectral range 1440–900 cm^{-1}. A spectral resolution of 4 cm^{-1} and a lateral resolution of 128×128 pixels were applied. The data-acquisition time for 32 scans with these parameters was approximately 80 s. The hyperspectral imager measured the emitted and reflected radiation of the painting from a distance of approximately 1 m. The field of view of each pixel was 0.69 mrad, and a total area of 8.8×8.8 cm^2 was investigated. In this study, the hyperspectral images were processed by the use of a linear filter with a Gauß kernel of 3×3 pixels with a width of 3 pixels.[14] The radiometric calibration was performed automatically by an internal active calibration system, which enabled the calculation of brightness temperature spectra (measured in Kelvin). The measurements were performed by illuminating the sample with an infrared radiation source. The source is controlled by a USB interface, which enables the user to control the radiant power. To minimize the exposure time of the analyzed painting, the source is equipped with an iris shutter, which opens only during data acquisition. During the data-acquisition time of approximately 80 s, the measured heating of the painting surface was 4–5 °C.

Point-analysis measurements were carried out with a portable Alpha-R spectrometer (Bruker Optics) equipped with a Globar Mid-IR source, a 30° interferometer, and a room-temperature DLaTGS detector. Sampling was carried out by an external reflectance module with specular optics (22°/22°); the sampled spot had a diameter of about 6 mm. A total of 200 interferograms were acquired in the spectral range 7500–375 cm^{-1} with a spectral resolution of 4 cm^{-1}.

© 2013 Wiley-VCH Verlag GmbH & Co. KGaA, Weinheim

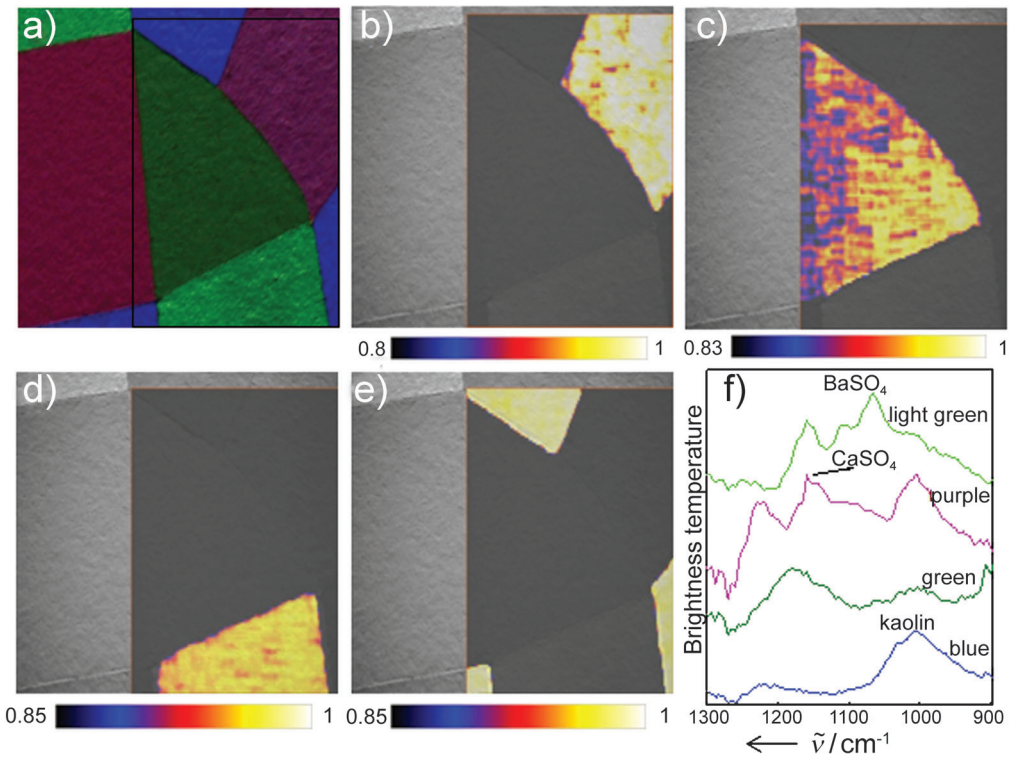

Figure 3. a) Color image of a portion of the painting *Sestante 10* by Burri. The black rectangle highlights the area investigated with the HI90 system (area III). b–e) Correlation images with reference spectra collected from the purple (b), dark-green (c), light-green (d), and blue areas (e). f) Reference spectra representative of the purple, dark-green, light-green, and blue areas.

Reflection spectra were compared directly with the brightness temperature spectra collected with the HI90 imager. A background correction was applied by using a reference spectrum for a gold flat mirror to represent the reflectance profile (R) expressed in the graphs as pseudoabsorbance, $\log(1/R)$.

Received: December 12, 2012
Revised: March 5, 2013
Published online: April 15, 2013

Keywords: analytical methods · chemical imaging · hyperspectral imaging · IR spectroscopy · paintings

[1] A. Romani, C. Clementi, C. Miliani, G. Favaro, *Acc. Chem. Res.* **2010**, *43*, 837 – 846.
[2] L. De Viguerie, P. Walter, E. Laval, B. Mottin, V. A. Solé, *Angew. Chem.* **2010**, *122*, 6261 – 6264; *Angew. Chem. Int. Ed.* **2010**, *49*, 6125 – 6128.
[3] G. Chiari, *Nature* **2008**, *453*, 159.
[4] F. Rosi, V. Manuali, T. Grygar, P. Bezdicka, B. G. Brunetti, A. Sgamellotti, L. Burgio, C. Seccaroni, C. Miliani, *J. Raman Spectrosc.* **2011**, *42*, 407 – 414.
[5] C. Miliani, F. Rosi, B. G. Brunetti, A. Sgamellotti, *Acc. Chem. Res.* **2010**, *43*, 728 – 738.
[6] F. Rosi, C. Miliani, C. Clementi, K. Kahrim, F. Presciutti, M. Vagnini, V. Manuali, A. Daveri, L. Cartechini, B. G. Brunetti, A. Sgamellotti, *Appl. Phys. A* **2010**, *100*, 613 – 624.
[7] C. Daffara, D. Ambrosini, L. Pezzati, D. Paoletti, *Opt. Express* **2012**, *20*, 14746 – 14753, and references therein.
[8] W. De Nolf, J. Dik, G. Van der Snickt, A. Wallert, K. Janssens, *J. Anal. At. Spectrom.* **2011**, *26*, 910 – 916.
[9] J. K. Delaney, J. Z. Zeibel, M. Thoury, R. Littleton, M. Palmer, K. M. Morales, E. R. de La Rie, A. Hoenigswald, *Appl. Spectrosc.* **2010**, *64*, 584 – 594.
[10] P. Ricciardi, J. K. Delaney, M. Facini, J. G. Zeibel, M. Picollo, S. Lomax, M. Loew, *Angew. Chem.* **2012**, *124*, 5705 – 5708; *Angew. Chem. Int. Ed.* **2012**, *51*, 5607 – 5610.
[11] M. Vagnini, C. Miliani, L. Cartechini, P. Rocchi, B. G. Brunetti, A. Sgamellotti, *Anal. Bioanal. Chem.* **2009**, *395*, 2107 – 2118.
[12] C. Miliani, F. Rosi, A. Daveri, B. G. Brunetti, *Appl. Phys. A* **2012**, *106*, 295 – 307.
[13] M. Spring, C. Ricci, D. A. Peggie, S. G. Kazarian, *Anal. Bioanal. Chem.* **2008**, *392*, 37 – 45.
[14] S. Sabbah, R. Harig, P. Rusch, J. Eichmann, A. Keens, J. Gerhard, *Opt. Eng.* **2012**, *51*, 111717.
[15] R. Harig, R. Braun, C. Dyer, C. Howle, B. Truscott, *Opt. Express* **2008**, *16*, 5708 – 5714.
[16] M. T. Doménech-Carbó, M. J. Casas-Catalán, ·A. Doménech-Carbó, R. Mateo-Castro, J. V. Gimeno-Adelantado, F. Bosch-Reig, *Fresenius J. Anal. Chem.* **2001**, *369*, 571 – 575.

 © 2013 Wiley-VCH Verlag GmbH & Co. KGaA, Weinheim